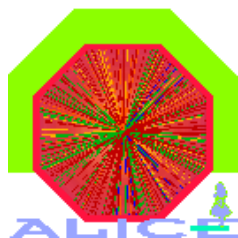


EUROPEAN ORGANIZATION FOR NUCLEAR RESEARCH  
European Laboratory for Particle Physics



**Internal Note/**

ALICE reference number

ALICE-INT-2005-003 version 1.0

Institute reference number

[-]

Date of last change

2005-01-07

**Techniques to estimate the intrinsic resolution of the ALICE  
Silicon Pixel Detector with application to 2003 beam test data**

**Authors:**

J.Conrad, P.Nilsson

**Abstract:**

In this note we present some novel techniques to estimate the intrinsic resolution of the ALICE Silicon Pixel Detector. The intrinsic resolution can be inferred from measured residual distributions knowing the contribution of the tracking error (the measurement error of the tracking) and multiple scattering. We present two methods for estimating the tracking error, one applicable to the linear case, the other one applicable to arbitrarily complicated tracking problems. The contribution of multiple scattering to the tracking error is calculated. The intrinsic resolution is obtained using a method which takes into account the fact that the intrinsic resolution is best parameterized by a uniform distribution. It is seen that the traditional approximation of Gauss subtraction seems sufficient. Finally, we present an interactive method applicable to the case where the resolution of the tracking detectors is initially unknown.

These techniques are applied to 2003 test beam data. We present estimates of the single pixel and double pixel resolution at zero tilt angle and for different detector thresholds.

## 1. Introduction

The intrinsic resolution of the ALICE Silicon Pixel Detector (SPD) is a very important ingredient to the tracking algorithms, since it determines the error on the reconstructed cluster coordinates. The intrinsic resolution is given by:

$$\sigma_{intrinsic} = \frac{d}{\sqrt{12}} \quad (1.1)$$

where  $d$  is the sensitive region in which a hit causes a pixel to fire. For clusters with only 1 fired pixel for example one could use as an approximation that  $d$  equals the width of the pixel. In general  $d$  will depend on the size of the cluster, the inclination angle and detector properties such as threshold.

A dedicated experiment to estimate the intrinsic resolution would use tracking devices with known resolution which in the best case is significantly better than the detector under study.

Since the estimate of the intrinsic resolution was not the main goal of previous test beams of the SPD, the tracking detectors used were of the same type as the detector under study. Thus the tracking devices did not only not have better resolution than the detector under study, but furthermore the resolution was not known.

In this note we present some techniques to arrive at an reliable estimate of the intrinsic resolution also under these sub-optimal conditions.

## 2. The 2003 SPD test beam

In 2002 and 2003, two test beam experiments (TB2002 and TB2003) were carried out at the H4 beam line at the CERN SPS. During TB2002, a 350 GeV/ $c$  positive beam with an intensity of  $10^4$  particles per spill was used, while a 158 A GeV/ $c$  indium beam with  $10^4$  ions per spill was used during TB2003 as well as a positive beam of 120 A GeV/ $c$ . For the heavy ion run, a lead target was used, while no target at all was used with the positive beams and the detectors were placed directly in the beam.

Several assemblies and ladders were tested and are further discussed in [1]. The study presented in this report is based on the the 2003 proton data.

The basic configuration during both test beams was to use four reference planes for track definition and then project the found tracks into a plane of study. The 2003 proton run setup is shown in figure 1. Due to the pixel dimension,  $50 \times 425 \mu m^2$ , two pixel planes were rotated  $90^\circ$  as compared to the others, in order to get a more rigid track definition. During the previous test beam in 2002, the geometry was the same for all planes (i.e. all planes had the long and short pixels in the same direction). It was then noticed that the track reconstruction suffered somewhat in especially the long pixel direction, which led to less well determined residuals. The rotation of the

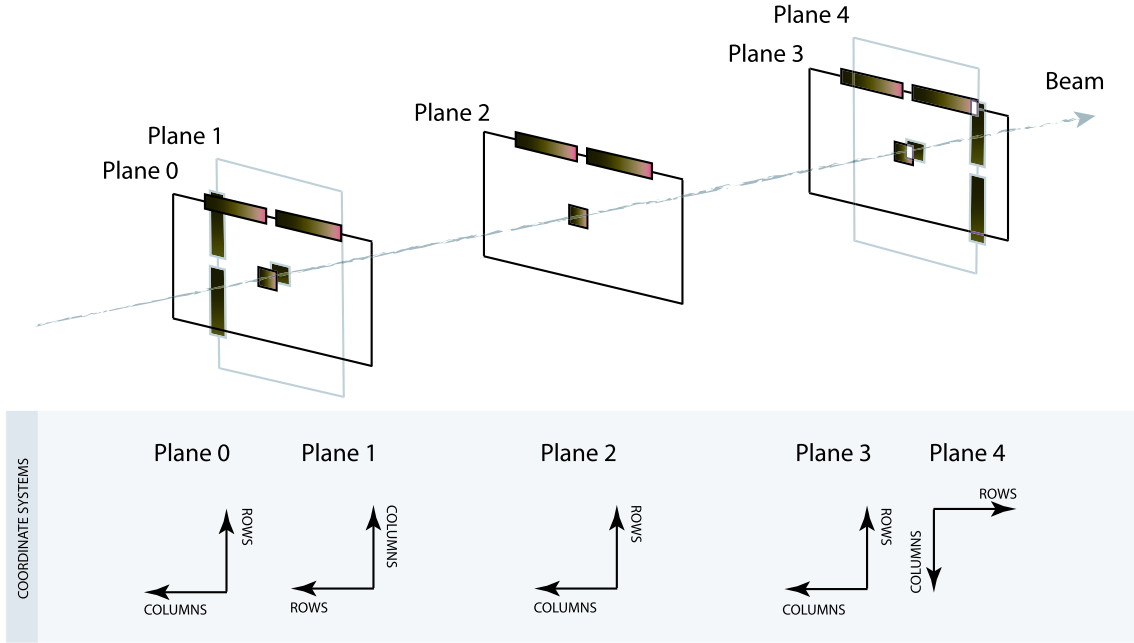


**Figure 1:** The 2003 proton run test beam setup. With a numbering of the planes ranging from 0 to 4, planes 1 and 4 are rotated 90° with respect to the other planes. For practical mounting reasons they were also mirrored.

planes in TB2003 helped the reconstruction, and the residual distributions got more well shaped in both directions.

The middle plane was placed on a remotely controlled XY-table that could move the plane in the X and Y directions as well as tilt it between 0°-45° with high precision. It is noteworthy that the plane under test had a 300  $\mu\text{m}$  sensor, whereas in the final ALICE configuration it will be 200  $\mu\text{m}$ .

### 3. Analysis

The analysis software is a complete stand-alone C++ package for decoding and reconstructing the raw data taken during the test beams and is run in two steps. The first step (*raw2root*) decodes the raw data and permanently convert it to ROOT files that are then stored on CASTOR. Besides decoding and event sorting it also performs the time consuming pixel clustering, i.e. grouping of neighboring fired pixels followed by a geometrical mean calculation and position error estimation, as well as removal of noisy pixels. The second step (*analyze*) reads the preprocessed ROOT files produced in the first step and performs a fast alignment<sup>1</sup> followed by track reconstruction.

<sup>1</sup>In the case of a focused proton beam. For data taken with an unfocused beam the analysis tool relies on externally calculated alignment.

The end result of the reconstruction is the hit<sup>2</sup> information of the plane of study (selectable, but is usually the middle plane) along with relevant information such as cluster sizes and residuals, which is stored in another ROOT file. This processed ROOT file is then analyzed in interactive ROOT sessions.

The details about the offline test beam software and its corresponding algorithms will be described in a later report.

### 3.1 Tracking

Tracks are formed by taking the hits in the four reference planes and fit their global coordinates to straight lines using the least square method, in the XZ- and YZ-planes. The plane of study is not used in the fitting. The position errors of the hits include multiple scattering which are discussed in section 3.5. A found track is projected into the plane of study and the nearest measured hit is identified. The measured and projected hit positions along with the size of the original pixel cluster is stored in the processed ROOT file for later analysis. The residual distributions, defined as the distances from the projected to the nearest measured hits, are calculated in a separate analysis macro.

### 3.2 Analyzed data

The study presented in this report is based on focused beam proton data, with the middle plane (the plane of study) in an upright position (tilt angle 0). Only events with one single hit per tracking plane were selected (typically 40% of all events with a focused beam). The requirement on the plane under study was either only 1 pixel clusters (in case of 1 pixel cluster resolution) or only 2 pixel cluster (in case of 2 pixel cluster resolution).

### 3.3 Data cleaning

Due to the selection criteria for the tracking planes (see previous section) we get a rather pure data sample. Several noisy pixels were removed from especially plane 1 and 4, although this didn't affect the overall data quality much because of the single hit criteria. The quality of the data is reflected in figure 2 which shows the  $\chi^2$ -distributions in both projection planes. Moving one reference plane slightly affects the  $\chi^2$ 's dramatically, which suggests a small contribution of the alignment error.

### 3.4 The tracking error.

In this section we present two (in this case equivalent) methods to estimate the tracking error. We consider a linear track fit:

$$f(z) = az + b \tag{3.1}$$

---

<sup>2</sup>A hit is in the remainder of the paper defined as the geometrical mean of the fired pixel coordinates belonging to the same cluster.

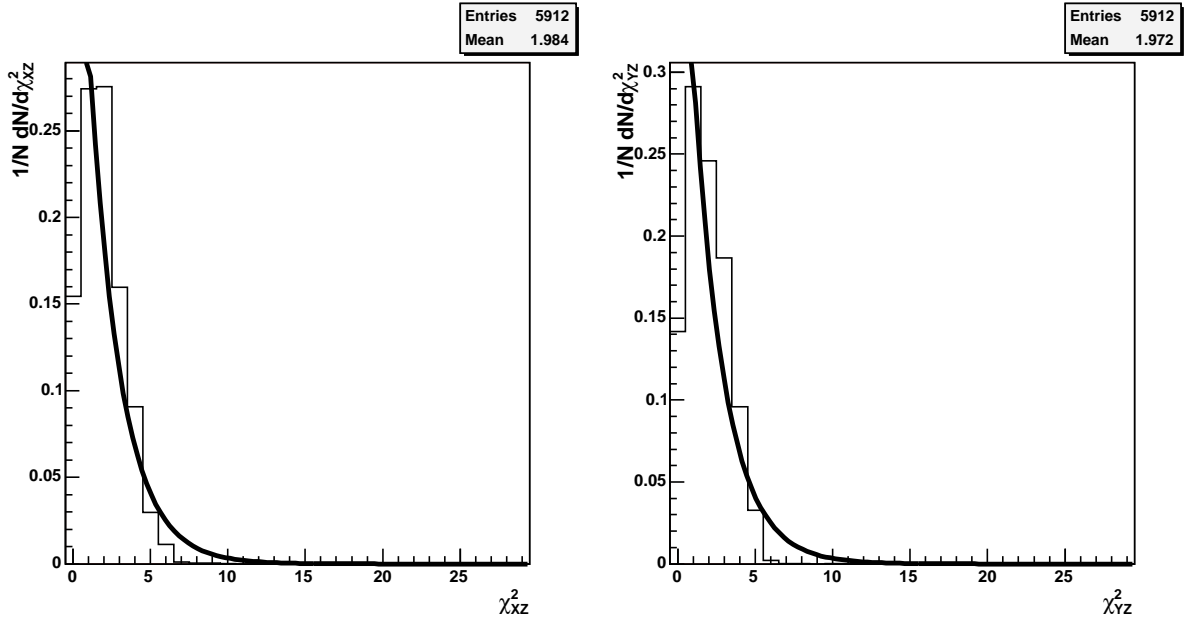


**Figure 2:**  $\chi^2$ -distributions in the XZ- and YZ-plane respectively. The laid-in functions are the theoretical  $\chi^2$ -distributions for two degrees of freedom.

To facilitate the problem, we define the coordinates system by setting  $z = 0$  in the tracking plane. Since we want to know the contribution of the error in the tracking to the residual coordinate only, this leads to the definition of the tracking error:

$$\sigma_{tracking} = \sigma_b \tag{3.2}$$

i.e. the estimate of the tracking error reduces to estimating the error in the fit parameter  $b$ . This reduction is a consequence of choosing the coordinate system in the above described way.

The behavior of the  $\chi^2$  as a function of the change of the parameter of interest can be used to estimate its error. The advantage of this method is that it is applicable to arbitrarily complicated track fitting problems. In the linear case that we are facing here, the method is equivalent to the inversion of the second derivatives of the least square function, i.e. the error can be easily calculated analytically. We present both methods. An interesting side remark is that both methods have recently been studied in a the more general context of confidence interval calculations and it has been shown that the  $\chi^2$  method has superior statistical properties [3].

### 3.4.1 The $\chi^2$ method

Confidence intervals on parameters (“errors”) can be obtained by using the likelihood

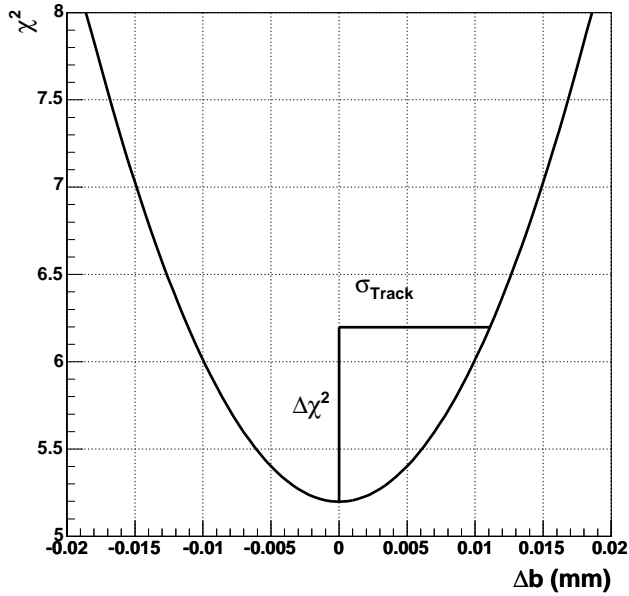


**Figure 3:** The recalculated  $\chi^2$  as a function of the change in tracking parameter  $b$ .

curve, see e.g. [2]. The calculated  $\chi^2$  can be used since asymptotically it holds:

$$\Delta\chi^2 \simeq -2 \log \left( \frac{L}{L_{max}} \right) \quad (3.3)$$

where  $\Delta\chi^2 = \chi^2 - \chi_{min}^2$ ,  $L$  is the likelihood function and  $L_{max}$  is the maximum of the likelihood function (corresponding to the minimum  $\chi^2$ ). In practice, the following steps have to be performed:

- standard reconstruction, retrieve  $\chi^2$
- translate track in the parameter for which the error is to be estimated (in our case the track parameter  $b$ )
- calculate  $\chi^2$  for the new track
- store new  $\chi^2$
- repeat in suitable parameter range

In this way, one constructs a curve  $\Delta\chi^2(\Delta b)$ . The error on the parameter can then be found by finding the points on the curve for which  $\Delta\chi^2 = 1$ , which correspond to standard  $1 \sigma$  errors. An example of the resulting curve is shown together with an illustration of the method in figure 3.

### 3.4.2 Analytic calculation

The analytic result is given by calculating the inverse error matrix which has as components the second derivatives of the least square function with respect to the track parameters. Defining coefficients:

$$A = \sum_i \frac{x_i}{\sigma_i^2} \quad B = \sum_i \frac{1}{\sigma_i^2} \quad C = \sum_i \frac{x_i^2}{\sigma_i^2} \quad (3.4)$$

the error in the parameter  $b$  is given by:

$$\sigma(b) = \frac{C}{BC - A^2} \quad (3.5)$$

More details on this calculation can be found in standard text books of data analysis such as [4].

### 3.5 Multiple scattering

The contribution to the position error from multiple scattering was estimated. For small deflection angles the Coulomb scattering distribution is roughly Gaussian and has a width

$$\theta_0 = \frac{13.6 \text{ MeV}}{\beta c p} z \sqrt{x/X_0} [1 + 0.038 \ln(x/X_0)] \quad (3.6)$$

where  $p$ ,  $\beta c$  and  $z$  are the momentum, velocity and charge number of the beam particle. The total thickness of the scattering medium,  $x/X_0$ , is taken as the sum of the individual material thicknesses. The material budget for the test plane is listed in table 1.<sup>3</sup>

<i>Material</i>	<i>Thickness (<math>\mu m</math>)</i>	<i>X<sub>0</sub> (cm)</i>
Al	10	8.9
Sensor (Si)	300	9.36
Bump bonds (60%Sn, 40%Pb)	0.385	0.95
Chip (Si)	725	9.36
Au	1	0.33
Cu	35	1.43
Glue (Epoxy)	75	44.37
PCB	1000	19.4

**Table 1:** Material budget for the test plane used during TB2003.

We have assumed scattering in each of the five planes and propagated test particles through the system. In each plane the scattering angle was drawn from a Gaussian

<sup>3</sup>The tracking planes had a sensor thickness of 200  $\mu m$ , while the chip thickness was 150  $\mu m$  in plane 0 and 3, and 725  $\mu m$  in plane 1 and 4.

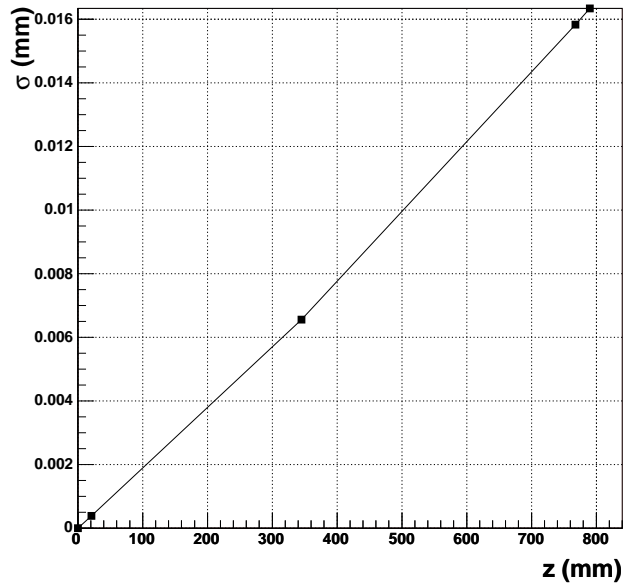


**Figure 4:** The multiple scattering errors vs. plane position along the beam.

distribution of width according to equation 3.6 and a mean equal to the previous plane’s scattering angle. The position of each test particle was calculated at each plane. The errors due to multiple scattering were taken as the widths of the position distributions. The widths of these distributions as a function of the plane position are shown in figure 4.

### 3.6 The intrinsic resolution

The residual distribution in the plane under study is a convolution of the intrinsic resolution of the detector with the tracking error. The intrinsic resolution of the detector is parameterized with a flat PDF and the tracking resolution is Gaussian. A traditionally used approximation is to obtain the intrinsic resolution of the detector by subtracting quadratically the tracking resolution from the  $\sigma$  of a Gauss fit to the residual distribution:

$$\sigma_{intrinsic}^2 = \sigma_{residual}^2 - \sigma_{tracking}^2 \quad (3.7)$$

This formula holds exactly in the case of convolution of two Gauss functions, while in the present case it has to be viewed as an approximation. We therefore present an alternative method which is based on a convolution of a Gauss distribution with a flat distribution.

#### 3.6.1 The Hypothesis Test Method

The Hypothesis Test Method consists of the following steps:



- produce a Toy MC, which convolves a Gauss distribution with  $\sigma_{tracking}$  and a flat distribution which is characterized by  $w$ , thus giving an intrinsic resolution of  $\frac{w}{\sqrt{12}}$
- loop over  $w$  and for each  $w$ , test the hypothesis:  
 $H_o$ : Data and simulated distribution are drawn from the same parent distribution
- Reject  $H_o$  if test-statistic is smaller than a critical value (in our case chosen to be 5 %)

The test statistics can hereby be chosen to be the most convenient for the problem at hand. We use the Kolmogorov-Smirnov (KS) test but also tested the  $\chi^2$  (Pearson's)-test. Both give comparable results. We also compare the results of the method with the common quadratic subtraction method. It can be seen that the quadratic subtraction method is a very good approximation. The 1 pixel intrinsic resolution is

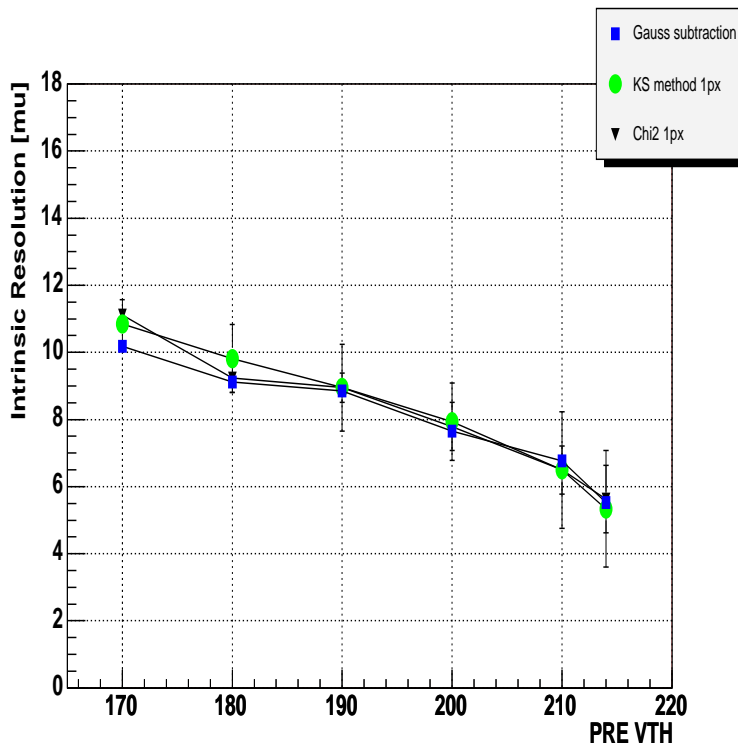


**Figure 5:** The intrinsic resolution in the shorter pixel coordinate as function of the threshold setting PRE-VTH (increasing PRE-VTH corresponds to decreasing threshold). The error bars correspond to the hypotheses that were not rejected by the KS test.

shown as a function of detector threshold for all three methods (Gauss subtraction, KS and  $\chi^2$  test) in figure 5. We also studied the 2 pixel cluster resolution, in which we required a cluster of 2 pixels (in either direction) for the plane under study.

Figure 6 compares the 1 pixel with the 2 pixel cluster intrinsic resolution. The result shows the expected behaviour: increasing the 1 pixel cluster resolution will lead to a decrease in the 2 pixel cluster resolution.

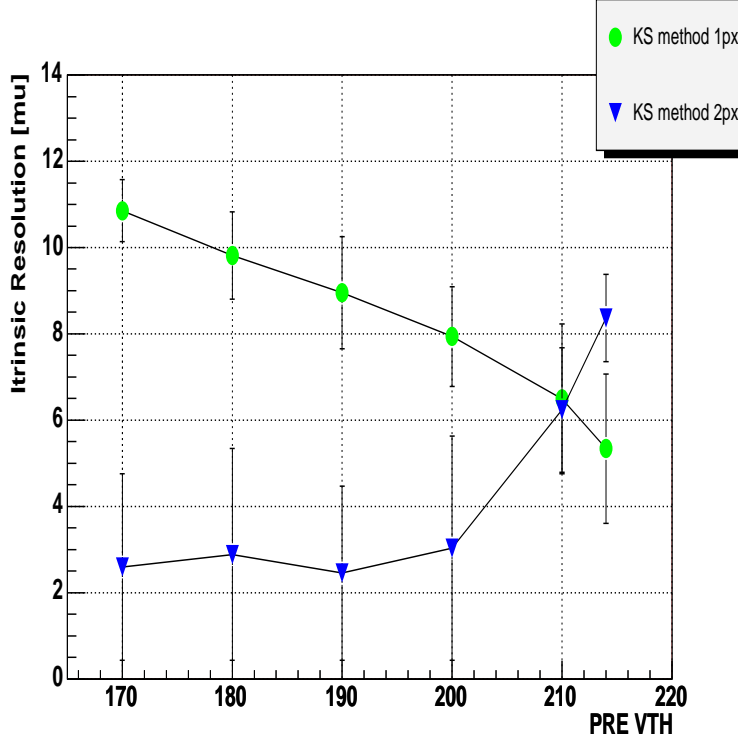


**Figure 6:** Intrinsic resolution for 1 and 2 pixel clusters as function of the threshold setting PRE-VTH (increasing PRE-VTH corresponds to decreasing threshold). The error bars correspond to the hypotheses that were not rejected by the KS test.

### 3.7 Iterative Method.

As we have seen in section 3.4, the tracking error is mainly depending on the errors on the cluster coordinates in the tracking planes. These errors are in turn determined by the intrinsic resolution we are trying to estimate. Therefore we follow an iterative scheme to obtain a better estimate of the intrinsic resolution. If the tracking planes were identical to the test plane, we could just take the found intrinsic resolution at the threshold at which the tracking planes were operated (in this case PRE-VTH 200). However, an additional complication arises due to the fact that the sensors in the tracking planes were not  $300 \mu m$  thick but  $200 \mu m$ . We therefore have to find the conditions (in particular the threshold setting) under which the intrinsic resolution found in the test plane is comparable to the one in the tracking planes. Since the probability to obtain 1 or 2 pixel clusters is proportional to the size of the sensitive region (which determines the intrinsic resolution), we use the ratio between 1 and 2 pixel clusters to infer the threshold at which the test plane has a similar intrinsic

resolution as the tracking planes. The ratio (between the test and tracking plane) of the ratio (of 1 and 2 pixel clusters) should be as close to 1 as possible. Figure 7 shows the deviation of the ratio of ratios from 1 as a function of threshold. It is concluded

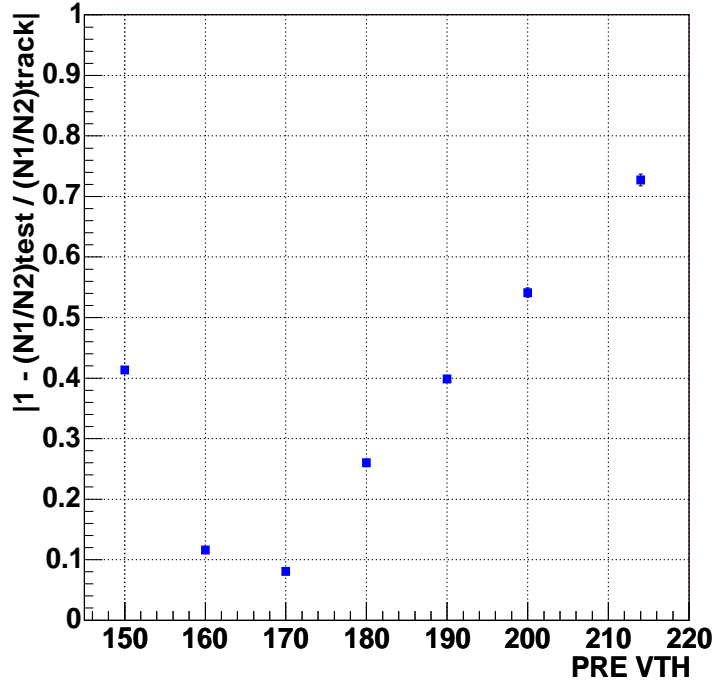


**Figure 7:** The deviation from 1 of the ratio of the ratios of 1 to 2 pixel clusters as a function of threshold.

that the ratio is closest to 1 at a threshold of PRE-VTH 170. Using the intrinsic resolution found at this threshold value, we calculate a new estimate of the tracking error and repeat the analysis. Usually we find fast convergence. Figure 8 shows the development of the estimate of the intrinsic resolution for different threshold settings as a function of the number of iterations. The tracking error estimate is also included. One sees that the initial tracking errors of  $12.3 \mu\text{m}$  in both directions changes to  $10.6 \mu\text{m}$  after six iterations. It is noteworthy that the error (defined as the hypotheses not rejected by the KS test) decreases with the number of iterations as well. Figure 9 shows the result for the intrinsic resolution of the pixel after one and five iterations. Also included is the result for the large pixel dimensions. In this case iterations are not necessary: the tracking error is negligible with respect to the intrinsic resolution. For completeness we show the resulting intrinsic resolutions for 1 and 2 pixel clusters as a function of threshold in figure 10.

We have summarized the main results of applying the presented techniques in table 2.

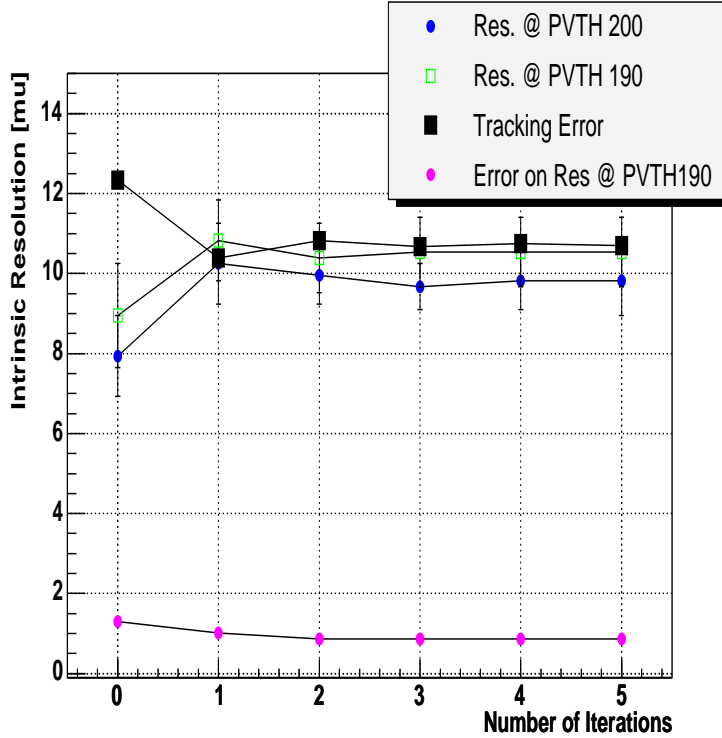


**Figure 8:** The found intrinsic resolution as a function of number of iterations for different thresholds. We also show the respective tracking error estimates well as the resulting error (defined as the hypotheses which were not rejected by the test).

<i>Quantity</i>	<i>Estimate (<math>\mu\text{m}</math>)</i>
$\sigma_{short}^{1px}$	$8.9 \pm 1.0$
$\sigma_{long}^{1px}$	$120.4 \pm 1.7$
$\sigma_{short}^{2px}$	$8.2 \pm 0.9$
$\sigma_{long}^{2px}$	$116.0 \pm 1.7$

**Table 2:** Selected intrinsic resolutions of the present study. All results are for a threshold of about 30 mV (PRE-VTH 210).

## 4. Conclusions & Outlook

In this note we present some techniques to estimate the intrinsic resolution of the ALICE SPD under sub-optimal conditions. We discuss simple (and powerful) methods to estimate the contribution of the measurement error and the multiple scattering. The inference of the intrinsic resolution is done in a way which takes into account

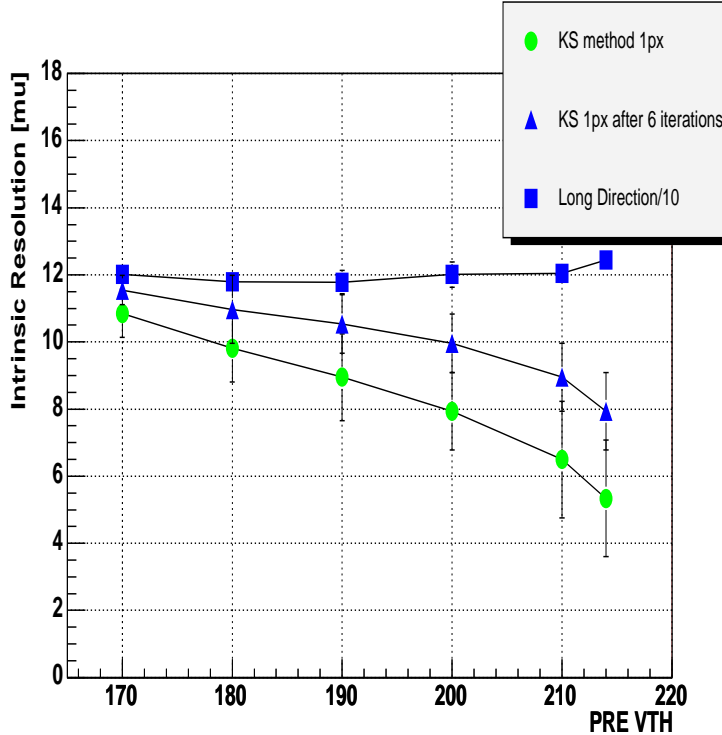


**Figure 9:** Intrinsic resolution with and without using the iterative method as function of the threshold setting PRE-VTH (increasing PRE-VTH corresponds to decreasing threshold).

the fact that the intrinsic resolution is uniform and it is seen that the traditional approximation of quadratic subtraction is good. Furthermore we devise an iterative scheme to compensate for the fact that the tracking devices did not have known intrinsic resolution. We obtain measurements of the intrinsic resolution for 1 and 2 pixel clusters at zero tilt angle as a function of threshold.

A parallel study [5] using a partly different approach obtains comparable results for the intrinsic resolution. We hope that the presented methods provide additional tools to use existing data to estimate the intrinsic resolution of the SPD for different cluster sizes and inclination angles relevant for ALICE. Obtaining these results is of high importance for the tracking algorithms used in ALICE and studies are under way.

## 5. Acknowledgements

Thanks to Domenico Elia and Romualdo Santoro for useful comments on an earlier draft. Thanks to Petra Riedler for information regarding the material budget.

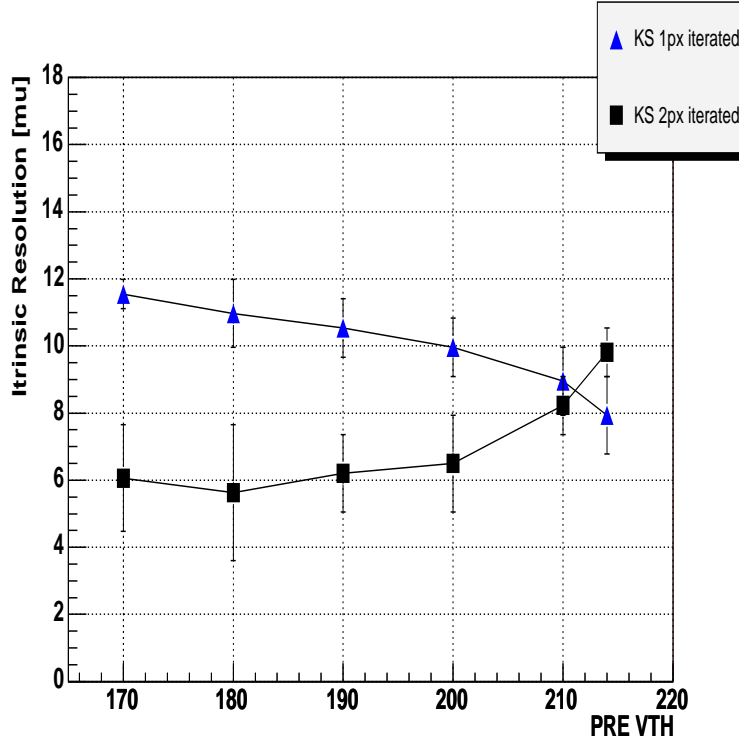


**Figure 10:** Intrinsic resolution for 1 and 2 pixel clusters as function of the threshold setting PRE-VTH (increasing PRE-VTH corresponds to decreasing threshold).

## References

- [1] P. Nilsson et al., Test Beam Performance of the ALICE Silicon Pixel Detector, Proceedings of the Vienna Conference on Instrumentation, Austria, February 2004, to be published in NIM A 2004.
- [2] F. James, ‘Interpretation of the Likelihood Function Around Its Minimum’, Computer Physics Communications **20** (1980) 29-35
- [3] W. Rolke, A. Lopez, J. Conrad and F. James, ‘Confidence Intervals in Presence of Nuisance Parameters’, physics/0403059, to be submitted to Phys.Rev.D (2004).
- [4] W.R. Leo, ‘Techniques for Nuclear and Particle Physics Experiments’, Springer-Verlag, (1994)
- [5] G.E. Bruno, M. Caselle, D. Elia, V. Manzari, F. Navach and R. Santoro, ‘Study of ALICE Silicon Pixel Detector performance in a beam test at SPD’, to be submitted as ALICE Internal NOTE.